

Borderline Magic Clustering: The Fabrication of Tetravalent Pb Cluster Arrays on Si(111)-(7 × 7) Surfaces

Shao-Chun Li, Jin-Feng Jia, Rui-Fen Dou, and Qi-Kun Xue

State Key Laboratory for Surface Physics, Institute of Physics, Chinese Academy of Sciences, Beijing 100080, People's Republic of China

Iskander G. Batyrev and S. B. Zhang

National Renewable Energy Laboratory, Golden, Colorado 80401, USA

(Received 15 May 2004; published 10 September 2004)

Well-ordered arrays of identical Pb clusters have been fabricated on a Si(111)-(7 × 7) substrate by the temperature-mediated surface clustering method. Interestingly, these clusters can easily transform into other forms when the growth temperature deviates slightly from the optimal values. In accord with experiments, first-principle total-energy calculations reveal several cluster structures centered on a mixed cluster model involving surface Pb and Si exchange. This borderline Pb/Si(111) system provides a unique, controlled way to study surface magic cluster formation and breakup dynamics.

DOI: 10.1103/PhysRevLett.93.116103

PACS numbers: 81.07.-b, 61.46.+w, 68.37.Ef, 68.43.Bc

The recently discovered ordered array of group-III metal clusters on Si(111)-(7 × 7) is a new form of artificial two-dimensional (2D) lattice, obtained by magic clustering on a periodic template of semiconductor surfaces [1–8]. The physics of such ordered cluster arrays is rich but has yet to be fully explored. For example, it was recently shown that the formation of alkali metal cluster arrays represents a classic example of gas-to-condensed matter phase transition in reduced dimensions [8]. To date, studies of the cluster arrays have mainly focused on the metal atoms distinctly different from substrate host atoms. It has not been possible to fabricate any tetravalent cluster arrays on Si despite their chemical and electronic similarities and despite that a Ge cluster array could be a holy grail for semiconductor nanoapplications. The dynamic process concerning the formation and breakup of any of the magic clusters is not understood, even though such a process could be vital to the eventual application of the cluster arrays, for example, in microelectronics, ultra-high density recording, and nanocatalysis.

In this regard, Pb on Si is unique because, while both have the same chemical valency, the 9% size mismatch between Pb and Si is large enough to make the Pb significantly different from Si. As a result, the miscibility gap between bulk Pb and Si is large. Also, Pb is a metal, making it suited for the current cluster deposition techniques. The structure of Pb/Si(111) by itself is also a subject of intensive study, revealing the $\sqrt{3} \times \sqrt{3}$, 3×3 , $\sqrt{7} \times \sqrt{3}$, 1×1 , and “devil’s staircase” phases [9–18]. It is noteworthy, however, that, despite many studies on the initial stage of Pb adsorption [19–23], a phase with an ordered cluster array has never been observed before.

In this Letter, we report that a well-ordered Pb cluster array—as a matter of fact the first for tetravalent—has been fabricated. However, both the substrate temperature

range (120 ± 20 °C) and the Pb coverage range at which ordering could occur are rather subtle, suggesting that among the applicable metals Pb could be at the borderline for array formation by the film deposition method. This borderline nature is also reflected by the observed multiple cluster structures, not seen in any other cluster arrays, which, as will be shown below, is of great fundamental importance for understanding metal-semiconductor interaction at the cluster level.

First-principles total-energy calculations are used to unveil the cluster structures. We found that a 6-Pb cluster (hereafter C6) is most stable and forms the basic unit of the ordered cluster array. In terms of the bonding topology, C6 resembles the 6-In cluster previously studied [1], but with little resemblance in the scanning tunneling microscopy (STM) appearance. Other metastable cluster, C5 and C7, are also determined both by energetic consideration and by the fact that the calculated STM images are in good agreement with experiment. This enables for the first time a study of the stability of C6 by releasing/attracting one or more Pb adatoms. For example, using isolated Pb on the surface as reservoir, it takes 1.9 eV to extract the Pb from the C6 cluster and 0.9 eV to place the Pb to the C6 cluster.

The experiments were carried out with an OMICRON variable-temperature STM system operated in ultrahigh vacuum ($\sim 5 \times 10^{-11}$ Torr). Details of this apparatus and the preparation of clean Si(111) surfaces have been described elsewhere [1,2]. High purity Pb(99.9999%) was evaporated from a tantalum boat by direct current heating. The substrate temperature was set from room temperature (RT) to ~ 200 °C, and the deposition rate was controlled at approximately 0.05 ML(monolayer)/min (1 ML = 7.84×10^{14} atoms/cm²). Chemically etched tungsten tips were used for scanning. All STM images

reported here were recorded at RT under a constant tunneling current of 20 pA.

Because adatom diffusion plays the pivotal role in epitaxial film morphology, frozen mobility usually leads to featureless configurations, while too fast diffusion suppresses the template effect of the substrate and leads to Pb agglomeration [24]. Delicate regulation of the substrate temperature is thus important in coordinating a kinetic pathway for the formation of ordered arrays. Figure 1 shows topographic STM images of an ordered, identical Pb cluster array by depositing ~ 0.1 ML Pb at $\sim 120^\circ\text{C}$. The Pb clusters occupy predominantly the faulted halves of the 7×7 unit cells (FHUCs), leaving the unfaulted halves of the unit cells (UFHUCs) nearly uncovered. The Pb C6 cluster appears in the filled state image (-1.0 V), as a pointed triangle with three bright central spots and three less bright tails [Fig. 1(a)], but only the three bright spots can be discerned [Fig. 1(b)] in the empty-state image ($+1.5$ V). The lateral distance between the central bright spots in Fig. 1(a) is determined to be 6.0 ± 0.5 Å, which is 1.7 Å smaller than the ideal spacing between Si rest atoms (7.7 Å). In other words, these spots are not exactly on top of the rest atoms, but are shifted towards the center. Note that the topological morphology here is completely different from either group-III or alkali metal clusters [1–4,8]. For example, the empty-state image of an In C6 cluster (inset) is a six bright-spot inverted triangle with respect to the underlying FHUC. Despite the qualitative differences, Pb coverage calibration suggests that each C6 contains 6 ± 1 Pb adatoms, which is the same as group-III and alkali metal clusters [1–8].

We have carried out extensive first-principles total-energy calculations to determine the cluster structures. Details of the methods have been reported elsewhere [1–4,8]. Cho and Kaxiras have previously showed [25] that there exist “attraction basins” in which isolated alkali metal adatoms could move nearly freely. For group-IV atoms such as Si and Ge, which prefer the bridge B_2 site

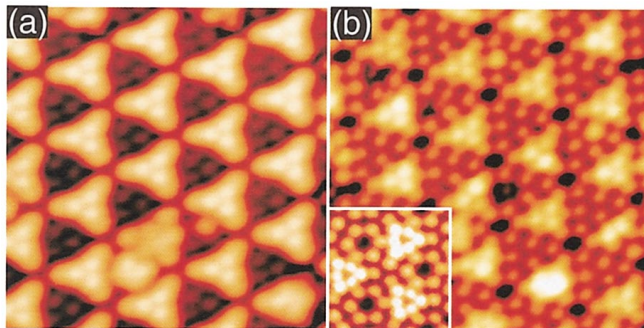


FIG. 1 (color). STM images ($11 \text{ nm} \times 11 \text{ nm}$) of the Pb cluster array on Si(111)-(7 \times 7). The bias voltages are (a) -1.0 V and (b) $+1.5$ V. The inset shows an empty-state STM image of an In₆ cluster.

between an adatom and a rest atom, the situation is, however, different. It takes about 2 eV to move from one B_2 site to another B_2 site through the T_1 site atop a rest atom and about 1 eV through the hollow H_3 site at the center of the HUCs. We find a similar energy curve for isolated Pb, although Pb is expected to be less reactive to Si than either Si or Ge. Taking the equilibrium B_2 structure, we have calculated several 3-Pb clusters (C3) with different Pb-Pb distance. However, not only is the number of atoms inconsistent with experiment but also the calculated binding energies are negligibly small due to large Pb/Pb separation. Several other models with three to six Pb atoms were also considered but none came out with energy nearly as low as B_2 . This prompted us to reconsider the original C6 model for all group-III clusters. The rationale was that C6 at least maximizes the number of covalent bonds, and Pb could exchange with isovalent Si during the growth so the STM images can still be significantly different from those in Refs. [1–4]. Figure 2(a) shows the fully optimized atomic structure of the minimum-energy Pb C6 model. The binding is indeed significant, -0.45 eV/Pb, when compared with six isolated Pb adatoms on the B_2 sites.

The calculated filled state image [Fig. 2(b) at -1.4 V] of the C6 model shows clearly that only six Pb adatoms in the FHUC are visible with the central three Pb significantly brighter than the corner ones. In the uncovered

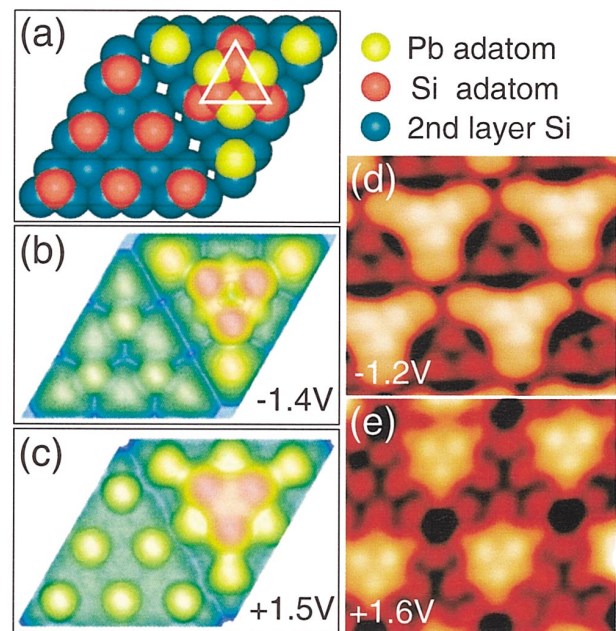


FIG. 2 (color). (a) Top view of the calculated C6 model. The inverted triangle designates the original In₆ structure without the Pb/Si exchange. Calculated (b) filled and (c) empty-state STM images using the C6 model in (a) with bias voltage -1.4 and $+1.5$ V, respectively. Red is close to and blue is away from the surface. Atomically resolved STM images obtained at (d) -1.2 V and (e) $+1.6$ V are also shown.

UFHUC, the three Si rest atoms are also visible, whereas the visibility of the six Si adatoms has been strongly suppressed. On the other hand, the calculated empty-state image [Fig. 2(c) at +1.5 V] shows that (i) the three central Pb adatoms remain bright, (ii) the Si adatoms located at the center of the FHUC become visible, and (iii) those Pb adatoms on the corners are darkened considerably. In the uncovered UFHUC, the image is indifferent from that of a clean 7×7 surface. Figures 2(d) and 2(e) show the atomically resolved STM images obtained at -1.2 and $+1.6$ V, respectively. Both theoretical images in Figs. 2(b) and 2(c) agree with experiment remarkably

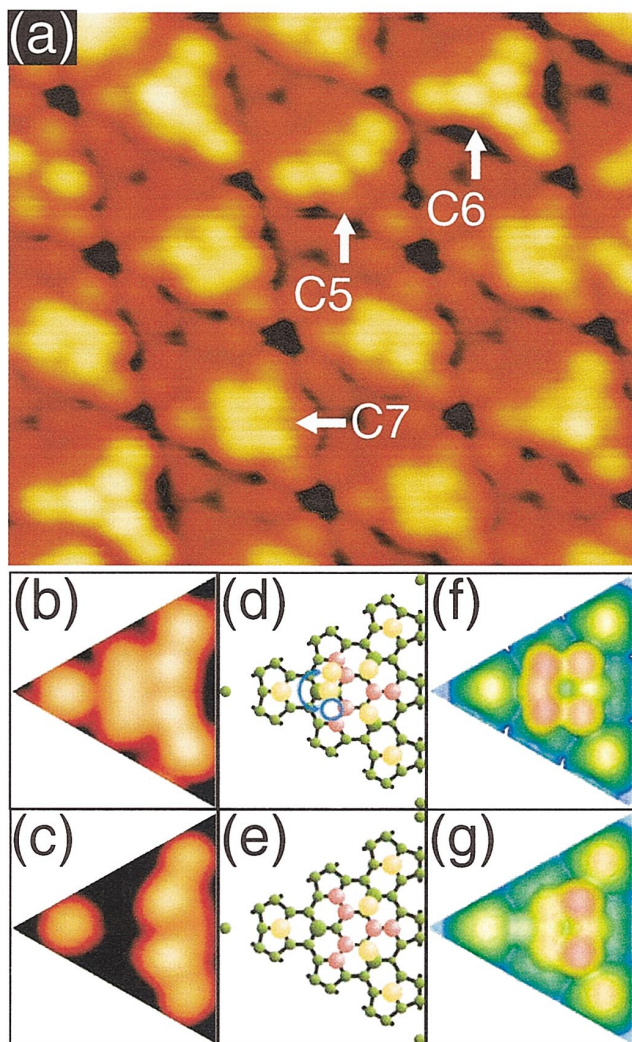


FIG. 3 (color). (a) Filled state STM image ($9 \text{ nm} \times 9 \text{ nm}$) for the adatoms, but green for second layer Si. Labels C5, C6, and C7 indicate the three types of clusters. (b),(c) Atomically resolved STM images, and (d),(e) calculated atomic structures for C7 and C5, respectively. The blue circle in (d) represents the empty (mirror) bridge site of the additional Pb adatom, which is occupied in C8. (f),(g) Calculated filled state images at -1.4 V .

well. This establishes C6 as the model for the Pb clusters beyond just the energetic consideration.

The agreement between experiment and theory above hints strongly that Pb/corner Si exchange has indeed been promoted by the exothermic formation of the clusters, although a similar exchange has never been observed at our growth temperatures before in the absence of the cluster phase. Otherwise, the preference of the corner sites by Pb is quite universal. After annealing low $\sim 0.02 \text{ ML}$ Pb coverage samples at $\sim 200^\circ \text{C}$ for 2 min, we observed that the Pb clusters decomposed into individual Pb atoms replacing Si adatoms. A careful statistical analysis shows that the number density of the Pb atoms is nearly 6 times that of the original Pb clusters and Pb prefers corner adatom sites than central adatom sites by at least a ratio of 1.5 to 1.

Next, we explore the mysterious multiple cluster structures surrounding C6. The remarkable experimental fact is that a well-ordered array of Pb clusters could only form in a rather narrow substrate temperature window of $100\text{--}140^\circ \text{C}$. A small deviation from the optimal growth conditions will lead to the formation of more than two kinds of clusters [see Fig. 3(a)]. For example, decreasing the growth temperature by 20°C leads to the emergence of a second kind of Pb cluster, i.e., C7 in Fig. 3(b). The size and shape of C7 are rather similar to those of C6, except that one of the central spots is now elongated and appears blurry. While the C6 cluster has the threefold symmetry, the C7 cluster has only the mirror symmetry and is hence randomly oriented along all the three equivalent symmetry axes. Repeated scans using different tips show that the blurry barlike feature and the directional characteristics of the C7 are not due to some unexpected effect related to STM tip geometry. Moreover, clusters with one nominally missing Pb atom, i.e., C5 in Fig. 3(c), are also clearly seen in Fig. 3(a).

Figures 3(d) and 3(e) show the calculated atomic structure for C7 and C5, respectively. In C7, the extra Pb atom resides on a bridge site above the C6 cluster. The calculated energy is 0.26 eV/Pb lower than a Pb at the trans-

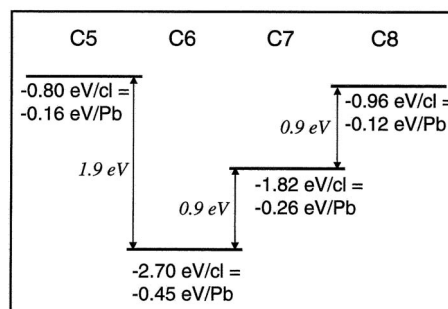


FIG. 4. Cluster (cl) energy versus cluster size. Energy per Pb is obtained by dividing the energy per cl by the number of atoms in the cluster. Isolated Pb atoms at the B_2 site define the energy zero.

port B_2 site, but is 0.19 eV/Pb higher than a Pb in a C6 cluster. We also calculated a C8 cluster by placing another Pb on the mirror site in Fig. 3(d) (denoted by a blue circle). Evidently, C8 is less stable than C7 but the energy is still -0.12 eV/Pb lower than B_2 . In either case, the energy required to add the extra Pb(s) to the cluster from a B_2 site (which could be considered as a reservoir for isolated Pb) is 0.9 eV per added Pb (see Fig. 4). In C5, one of the three central Pb adatoms is removed. The calculated energy is -0.16 eV/Pb lower than B_2 . The energy required to extract the Pb from C6 to form C5 is, however, large, 1.9 eV (Fig. 4). The fact that the energy per Pb for both C5, C7, and C8 are still significantly lower than that of B_2 suggests that the C6 cluster is rather stable and will not dissociate even when it loses one or traps one or two extra Pb atoms. Figures 3(f) and 3(g) show the calculated STM images for C7 and C5, respectively. In the calculation for C7, we have assumed that the added Pb is mobile enough to be displaced back and forth [as shown by the blue arrow in Fig. 3(d)] by the scanning tip to exhibit the barlike feature by average. We have also calculated the image for C8 and find it to be indistinguishable from that of averaged C7. Overall, the agreement with experimental images [see Figs. 3(b) and 3(c)] is good. By comparing theory with experiment, our results also reveal how a magic C6 cluster actually breaks initially: It does not happen at the corners, but rather at the edges, of the inverted triangle shown in Fig. 2(a).

Our calculated results suggest that the formation of the C6 cluster arrays could not be dictated entirely by surface thermodynamics, as it would suggest a gradual increase of the C5 and C7 (C8) densities at elevated temperatures in contradiction with experiment. The large energy barrier of at least 1.9 eV to extract a Pb from C6 is also difficult to overcome at the growth temperature (around 120 °C). Hence, the statistical distribution of the Pb clusters is controlled largely by growth kinetics. This is in contrast to group-III metals for which the temperature window for array formation is considerably larger because of smaller kinetic barriers: the diffusion barrier out of the attraction basins for group-III atoms (about 0.5 eV) is only half of that for group-IV atoms (about 1.0 eV). Electronic states of the clusters are another important factor. For example, in group-III clusters the dangling bonds of the six metal atoms in the inverted triangle are empty so the clusters are chemically “inert.” However, in group-IV clusters, the corresponding dangling bonds ideally should be half occupied to accommodate the six extra electrons. Thus, it should be much easier for passing-by adatoms to be captured to form either C7 or C8.

In summary, we have presented the first evidence for temperature-mediated tetravalent cluster formation and ordering on the Si(111)-(7 × 7) template. Well-ordered Pb

cluster arrays are obtained. Outside a narrow growth temperature (± 20 °C) and Pb coverage window, however, cluster uniformity decreases quickly due to the formation of other forms of clusters. First-principles total-energy calculations reveal the atomic structures of the clusters and the calculated STM images based on the models are in good agreement with experiment. By exploring the formation and breakup dynamics of the Pb clusters, we suggest that in general the low surface diffusivity and high chemical reactivity of the tetravalent adatoms on Si(111)-(7 × 7) must be overcome in order to fabricate their cluster arrays.

Work at IoP is supported by National Science Foundation and Ministry of Science and Technology of China. Work at NREL was supported by U.S. DOE/BES and DOE/EERE under Contract No. DE-AC36-99GO10337 and by DOE/NERSC for MPP time.

-
- [1] J. L. Li *et al.*, Phys. Rev. Lett. **88**, 066101 (2002).
 - [2] J.-F. Jia *et al.*, Phys. Rev. B **66**, 165412 (2002).
 - [3] J.-F. Jia *et al.*, Appl. Phys. Lett. **80**, 3186 (2002).
 - [4] J.-F. Jia *et al.*, Mod. Phys. Lett. B **16**, 889 (2002).
 - [5] M. Y. Lai and Y. L. Wang, Phys. Rev. B **64**, 241404 (2001).
 - [6] V. G. Kotlyar *et al.*, Phys. Rev. B **66**, 165401 (2002).
 - [7] H. H. Chang *et al.*, Phys. Rev. Lett. **92**, 066103 (2003).
 - [8] K. Wu *et al.*, Phys. Rev. Lett. **91**, 126101 (2003).
 - [9] M. Hupalo, J. Schmalian, and M. C. Tringides, Phys. Rev. Lett. **90**, 216106 (2003).
 - [10] B. Brochard *et al.*, Phys. Rev. B **66**, 205403 (2002).
 - [11] O. Custance *et al.*, Surf. Sci. **482-485**, 1399 (2001).
 - [12] J. Slezák, P. Mutombo, and V. Cháb, Phys. Rev. B **60**, 13328 (1999).
 - [13] L. Seehofer, G. Falkenberg, D. Daboul, and R. L. Johnson, Phys. Rev. B **51**, 13503 (1995).
 - [14] I.-S. Hwang, R. E. Martinez, C. Liu, and J. A. Golovchenko, Surf. Sci. **323**, 241 (1995).
 - [15] X. Tong, K. Horikoshi, and S. Hasegawa, Phys. Rev. B **60**, 5653 (1999).
 - [16] B. Ressel, J. Slezák, K. C. Prince, and V. Cháb, Phys. Rev. B **66**, 035325 (2002).
 - [17] D. Tang, H. E. Elsayed-Ali, J. Wendelken, and J. Xu, Phys. Rev. B **52**, 1481 (1995).
 - [18] E. Ganz *et al.*, Phys. Rev. B **43**, 7316 (1991).
 - [19] J. M. Gómez-Rodríguez *et al.*, Phys. Rev. Lett. **76**, 799 (1996).
 - [20] J. Slezák, V. Cháb, Z. Chvoj, and P. Mutombo, J. Vac. Sci. Technol. B **18**, 1151 (2000).
 - [21] J. M. Gómez-Rodríguez, J.-Y. Veuillen, and R. C. Cinti, J. Vac. Sci. Technol. B **14**, 1005 (1996).
 - [22] Ph. Sonnet, L. Stauffer, and C. Minot, Surf. Sci. **407**, 121 (1998).
 - [23] O. Custance *et al.*, Phys. Rev. B **67**, 235410 (2003).
 - [24] Z. Zhang and M. G. Lagally, Science **276**, 377 (1997).
 - [25] K. Cho and E. Kaxiras, Europhys. Lett. **39**, 287 (1997).